# A Hybrid Artificial Neural Networks–Aspen Plus Framework for $CO_2$ Enhanced Biomass Gasification and Gas Turbine Performance

Rajendran Chandran[a], Amornchai Arpornwichanop[b], Jirat Mankasem[c], Long T. Duong[d], Anh N. Phan[e] and Phuet Prasertcharoensuk[a,b*]

[a] Department of Chemical Engineering, Faculty of Engineering, Chulalongkorn University, Bangkok 10330, Thailand

[b] Center of Excellence in Process and Energy Systems Engineering, Department of Chemical Engineering, Faculty of Engineering, Chulalongkorn University, Bangkok 10330, Thailand

[c] Faculty of Engineering at Kamphaeng Saen, Kasetsart University, Nakhon Pathom 73140, Thailand

[d] School of Engineering, Lancaster University, Lancaster LA1 4YW, United Kingdom

[e] School of Engineering, Newcastle University, Newcastle upon Tyne NE1 7RU, United Kingdom

* Corresponding author: phuet.p@chula.ac.th

## Abstract

Concerns over climate change and fossil fuel dependency have intensified the development of renewable energy and sustainable energy globally. However, conventional mechanistic models often struggle to capture the complex nonlinear behavior of integrated gasification and turbine systems, limiting their predictive accuracy and suitability for real-time applications. This study presents a hybrid modeling framework that integrates a two-stage biomass gasification and gas turbine model with artificial neural networks (ANNs) to enhance prediction accuracy for integrated biomass-to-power performance. More than 5,000 simulation cases were generated using a parametric grid sampling strategy and validated against experimental data from the literature to ensure model fidelity. Spearman's rank correlation analysis identified the air flow rate and the carbon dioxide ($CO_2$)-to-fuel ratio as the most influential parameters. The optimized ANN models achieved coefficients of determination ($R^2$) exceeding 0.99 and root mean square errors (RMSE) below 5%, substantially outperforming conventional modeling approaches. The proposed hybrid ANN–Aspen Plus framework enables rapid and reliable performance prediction, facilitates real-time optimization, and promotes carbon dioxide ($CO_2$) utilization in advanced biomass-to-power systems.

**Keywords:** Biomass gasification; Syngas; Artificial Neural Network; Carbon Dioxide Utilization

## 1. Introduction

The growing urgency to mitigate climate change, strengthen energy security, and lessen reliance on fossil fuels has intensified global interest in sustainable energy technologies. Among them, biomass, particularly lignocellulosic residues and waste, has emerged as a promising feedstock for renewable energy production because of its abundance, renewability, and near-carbon-neutral nature [1]. Currently, biomass contributes more than 10% of global primary energy and offers substantial potential for decentralized energy systems and fossil-fuel substitutions [2-3]. Biomass can be thermochemically converted into energy carriers such as hydrogen, heat/electricity and synthesis gas (syngas) via pyrolysis, combustion, and gasification [4–5]. Gasification is especially attractive, as it produces syngas/hydrogen that can be used for electricity generation, synthetic fuels, and value-added chemicals. Accurate modelling of the gasification process is therefore essential for improving process efficiency, minimizing experimental costs, and facilitating scale-up.

Conventional modelling approaches including equilibrium, kinetic, and computational fluid dynamics (CFD) models have been widely applied. However, each approach has notable limitations. For example, equilibrium models are simple but rely on idealized assumptions [6–7]; kinetic models are more accurate but require detailed mechanisms, which are difficult to obtain for diverse feedstocks and these kinetic data are often specifically designed and validated for particular reactor types and operating conditions [8]; and CFD models offer high spatial fidelity but at prohibitive computational cost, making them unsuitable for real-time control [9–10] a key bottleneck for advanced process-control platforms. These limitations have driven the adoption of machine learning (ML) techniques, particularly artificial neural networks (ANNs), which can model nonlinear, multivariable relationships directly from input data. Recent studies have employed artificial neural networks (ANNs) to predict syngas properties from biomass gasification across a wide range of operating conditions including temperature, pressure, gasifying-agent ratios and diverse feedstock compositions [11–13]. However, most ANN-based studies only focused on predicting either gasification performance or syngas yield, without considering the downstream energy conversion stage (e.g. gas turbines) and the results achieve only moderate predictive accuracy ($R^2$ around 0.95, RMSE > 10%), which limits their applicability in fully integrated biomass-to-power systems.

Gasifying agent also significantly affects the properties of the product gas. Although air is the cheapest and most common gasifying agent for biomass gasification, the product gas has low calorific value (4-6 MJ/$Nm^3$) [14] and contains up to 55 mol% of $N_2$, which requires a nitrogen separation process leading to an increase in capital and operational costs of the process [15]. Steam can produce high calorific value gas (15-20 MJ/$Nm^3$) with 44-49 mol% $H_2$ [16]. However, the main disadvantage of using steam as a gasifying agent is that it is energy intensive to generate steam, causing a reduction in process efficiency [17]. $CO_2$ has recently emerged as a reactive gasifying agent for biomass gasification to obtain high quality syngas, because it promotes the Boudouard and dry reforming reactions [18–20], yet its effect remains under explored in ANN frameworks, and no study has coupled $CO_2$-assisted gasification with gas turbine performance in a single predictive step. Utilization $CO_2$ as a carbon source not only enhances syngas quality (increasing $H_2$ and CO yields) but also supports global decarbonization strategies, e.g. national net-zero targets. Despite these advantages, the role of $CO_2$ in ANN-based gasification frameworks remains underexplored, and no study has yet coupled $CO_2$-assisted gasification with gas turbine performance in a unified predictive model.

Therefore, this study aims to: (i) develop a comprehensive Aspen Plus model of $CO_2$-enhanced biomass gasification integrated with gas turbine cycle over a wide range of operating conditions and the modelling results was validated using experimental data available in literature (ii) quantify the influence of key variables using Spearman's rank correlation and (iii) to train and validate ANN surrogates that accurately replicate on both gasifier and gas-turbine outputs with $R^2 > 0.98$ and RMSE < 5%. The study will open up the opportunities for real-time optimization, advance the digital transformation of biomass-to-power systems and utilization of $CO_2$ as a carbon source for energy production, contributing significantly to the environmental footprint and sustainability of the process as well as providing alternative carbon capture and storage techniques.

## 2. Methodology

A sequential hybrid modeling framework was adopted in this study. First, a mechanistic, thermodynamically consistent process model was developed in Aspen Plus to generate a high-quality and physically robust dataset. Subsequently, this dataset was used to train and validate

artificial neural network (ANN) surrogate models implemented in Python, enabling rapid and real-time prediction of system performance.

**2.1 Biomass gasification model**

The biomass gasification process was modeled in Aspen Plus V12.1 (Figure 1) using a two-stage approach. This two-zone configuration enables a more accurate representation of the complex physicochemical processes occurring during gasification and has been adopted in several recent simulation studies to improve model fidelity. The model comprises two distinct stages: a pyrolysis zone (PYRO), which simulates the thermal decomposition of biomass into char and volatiles, and a gasification zone (OXI+RED), which encompasses both oxidation and reduction reactions in the gas phase [21]. The pyrolysis zone was implemented using the RYIELD reactor block, allowing user-defined decomposition based on the elemental composition of the feedstock. Volatile products generated in this stage include both condensable species (e.g., tars, water) and non-condensable gases (e.g., CO, $H_2$, $CH_4$, $CO_2$), which are crucial for downstream application.

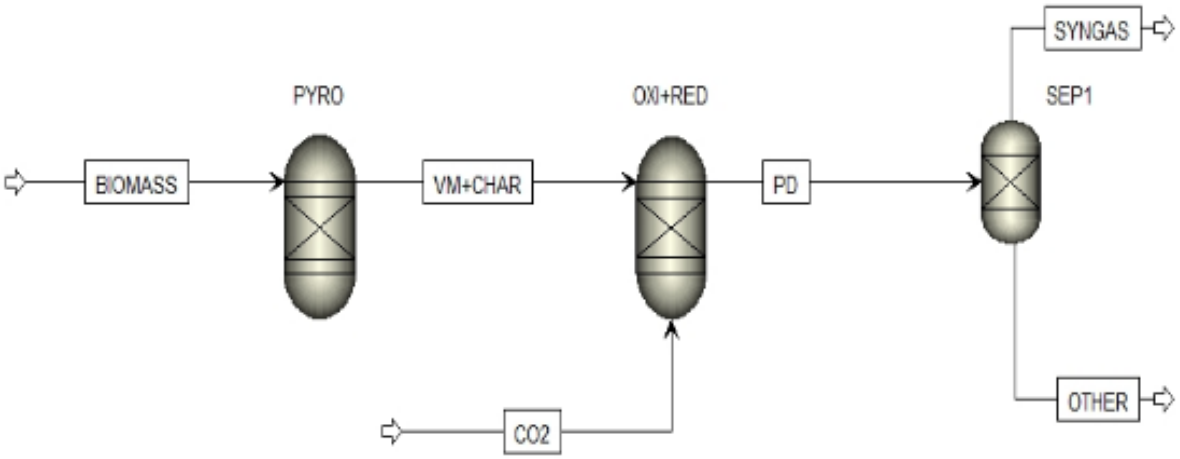


**Figure 1:** Simulation model of a two-stage biomass gasification process

The gasification zone was modeled using a single RGibbs reactor, which determines the equilibrium product distribution by minimizing the total Gibbs free energy of the system. This equilibrium-based approach is widely used in gasification simulations due to its robustness in handling complex reaction networks and its ability to accommodate diverse biomass compositions [22–24]. The model inputs include the elemental composition of the biomass (C, H, O, N, and S)

and key operating parameters such as reactor temperature and the $CO_2$-to-biomass ratio. Although the RGibbs approach does not explicitly account for kinetic limitations or intermediate species such as tars, thereby leading to a known tendency to overestimate $H_2$ and CO yields relative to real reactors this formulation was selected for its reliability, robustness, and general applicability in the absence of detailed kinetic data. Thermodynamic properties of vapor-phase species were calculated using the Peng–Robinson equation of state. For non-conventional solid components such as char and ash, the DCOALIGT and HCOALGEN property models were employed, in accordance with standard practice in coal and biomass gasification modeling [25]. Throughout the simulation framework, steady-state mass and energy conservation were strictly enforced to ensure that the dataset generated for ANN training is thermodynamically consistent and physically meaningful.

To estimate thermodynamic properties accurately, the Peng–Robinson equation of state was applied to vapor-phase species. For non-conventional solid components such as char and ash, the DCOALIGT and HCOALGEN models were employed, in line with standard practices in coal and biomass modeling [25]. Throughout the simulation framework, strict adherence to steady-state mass and energy conservation was enforced to ensure that the ANN training dataset reflects physically consistent thermodynamic behavior.

To validate the reliability of the Aspen Plus model, simulation results were benchmarked against experimental data reported in the literature for representative biomass feedstocks, including wood chips and rice husk [21,23]. The selected experimental cases correspond to autothermal gasification operated with air/$CO_2$ as the gasifying agent, at reactor temperatures in the range of 800–900 °C and under atmospheric pressure. In the present work, these operating conditions, together with the reported elemental compositions of the biomass feedstocks, were explicitly reproduced in Aspen Plus to ensure a consistent and meaningful basis for comparison between simulations and experiments. Table 1 presents a side-by-side comparison of the predicted and experimental syngas compositions for the major species ($H_2$, CO, $CO_2$, and $CH_4$), together with the corresponding relative errors. The results show that the deviations for the dominant syngas components ($H_2$, CO, and $CO_2$) remain within 4–7%, while the deviation for $CH_4$ is below 3%. The average absolute deviation for the major syngas species is therefore below 7%, demonstrating that the model satisfactorily captures the dominant thermodynamic trends

governing biomass gasification and is sufficiently accurate for dataset generation and subsequent ANN training.

**Table 1:** Validation of Aspen Plus model results against experimental data.

| Component (mol%) | Experimental Data [21, 23] | Aspen Plus Model Results | Relative Error (%) |
|---|---|---|---|
| Hydrogen ($H_2$) | 18.5 | 19.6 | 6.2% |
| Carbon Monoxide (CO) | 22.1 | 23.4 | 5.8% |
| Carbon Dioxide ($CO_2$) | 12.3 | 11.8 | 4.1% |
| Methane ($CH_4$) | 1.8 | 1.9 | 2.8% |

### 2.2 Gas turbine model

The gas turbine system was modeled in Aspen Plus V12.1 by integrating three key components: an air compressor, a combustion reactor, and a gas turbine expander, as shown in Figure 2. This configuration replicates the structure of a typical Integrated Gasification Combined Cycle (IGCC) system [26,27]. The air compressor increases the pressure of ambient air before it enters the combustion chamber. To account for realistic mechanical and aerodynamic losses, the isentropic efficiencies of the air compressor and the gas turbine expander were set at 85% and 90%, respectively. The combustion chamber was simulated using an RGibbs reactor block, which determines the equilibrium composition of combustion products by minimizing Gibbs free energy. This approach is well-suited for systems involving complex reaction pathways and unknown kinetics, enabling reliable estimation of flue gas composition. The air-to-fuel ratio was adjusted to meet the stoichiometric combustion requirements of biomass-derived syngas, ensuring complete oxidation and accurate thermal energy prediction. Mechanical losses during shaft power transmission were incorporated to reflect practical power generation constraints. The resulting high-temperature combustion gases were then expanded through the gas turbine to generate mechanical work, which was subsequently converted to electrical power.

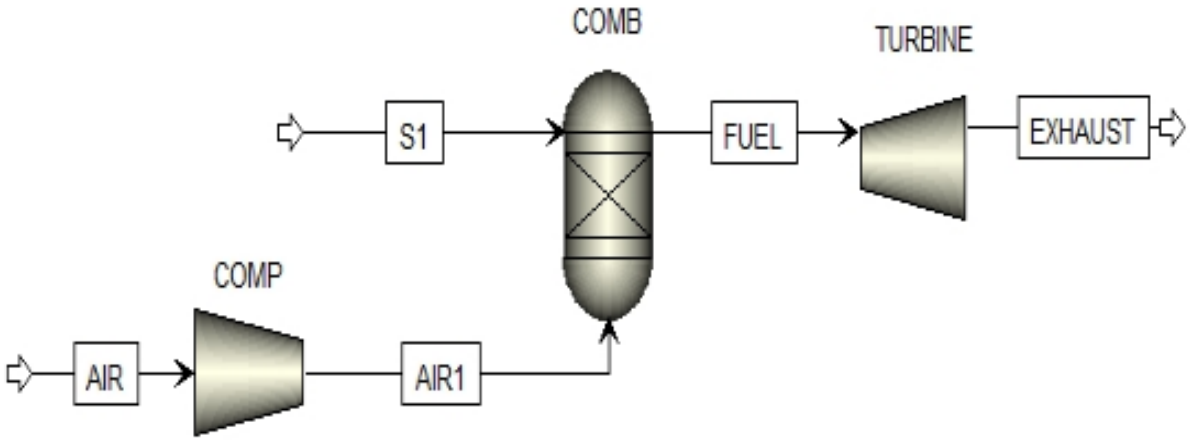


**Figure 2:** Simulation model of a gas turbine system

The thermodynamic behavior of the working fluid was modeled using the Peng–Robinson equation of state, which is suitable for simulating non-ideal gas behavior across varying pressure and temperature conditions. Key simulation outputs, including turbine exhaust temperature and mass flow rate, were cross-validated against reported data for small-to-medium-scale gas turbine systems to ensure physical consistency and model reliability. The primary outputs of the thermodynamic model—namely turbine power output and air mass flow rate were selected as target variables for training and validating the artificial neural network (ANN) models, given their direct relevance to system efficiency, operational flexibility, and load response characteristics. To maintain thermodynamic consistency, all system components were modeled under steady-state conditions based on the principles of mass and energy conservation. The overall mass balance of the gasification system is expressed as:

$$\sum m_{(in)} = \sum m_{(out)}$$

$$m_{(biomass)} + m_{(air)} + m_{(CO_2)} = m_{(syngas)} + m_{(residue)}$$

The energy balance across the gasifier is formulated as:

$$\dot{Q} - \dot{W} = \sum m_{(out)}\, h_{(out)} - \sum m_{(in)}\, h_{(in)}$$

where h denotes the specific enthalpy of each stream. For the autothermal gasifier, heat transfer to the surroundings is neglected, and the system is assumed to operate under adiabatic conditions ($\dot{Q} = 0$).

The net shaft power generated by the gas turbine system is calculated from the balance between the turbine expansion work and the compressor work requirement:

$$W_{(net)} = \eta_{\dot{m}}(m_{(gas)}\Delta h_{(turbine)} - \dot{m}_{(gas)}\Delta h_{(compressor)})$$

where $\dot{m}_{gas}$ is the working-gas mass flow rate, $\Delta h_{turbine}$ represents the specific enthalpy drop across the turbine, $\Delta h_{compressor}$ denotes the specific enthalpy rise across the compressor, and $\eta_m$ is the mechanical efficiency of the gas turbine shaft.

A summary of the mass and energy balance parameters used for the hybrid framework is provided in Table 2.

**Table 2.** Summary of Mass and Energy Balance Parameters for the Hybrid System.

| Component | Mass Balance | Energy Balance | Efficiency Parameters |
|---|---|---|---|
| Gasifier | $m_{in}$ ... syngas | $\sum(n_i \bar{h}_i)_{in} = \sum(n_j \bar{h}_j)_{out}$ | Thermodynamic Equilibrium |
| Combustor | $m_{syn}$ ... air = $m_{flue}$ | $LHV_{syn}$ ... syn ... comb | $\eta_{comb}$ = 98% |
| Turbine | $m_{in}$ ... out | $W_t$ =m.C ... p $\cdot \Delta T$ | $\eta_{is} = 90\%$; $\eta_m = 98\%$ |

### 2.3 Artificial Neural Network (ANN) Modeling

Two artificial neural network (ANN) models were developed in Python v3.10.12; the overall modeling workflow is shown in Figure 3. The first ANN model was designed to simulate biomass gasification model (Figure 3a), while the second was constructed to predict gas turbine performance (Figure 3b). Both models were implemented using the TensorFlow and Keras libraries [28]. Aspen Plus was coupled with Python through the COM (Component Object Model) automation interface, which enables external control of Aspen Plus from Python scripts. This interface was used to automatically modify input parameters, execute batch simulations, and extract key output variables. The resulting dataset was then parsed, cleaned, and directly used for ANN training and validation, thereby enabling a fully automated simulation–machine learning workflow. The ANN models were trained on data generated from the Aspen Plus simulations described in Sections 2.1 and 2.2, which were themselves validated against experimental data from the literature. This sequential validation strategy represents a robust hybrid modeling approach, in which the ANN serves as a real-time surrogate for a validated mechanistic model.

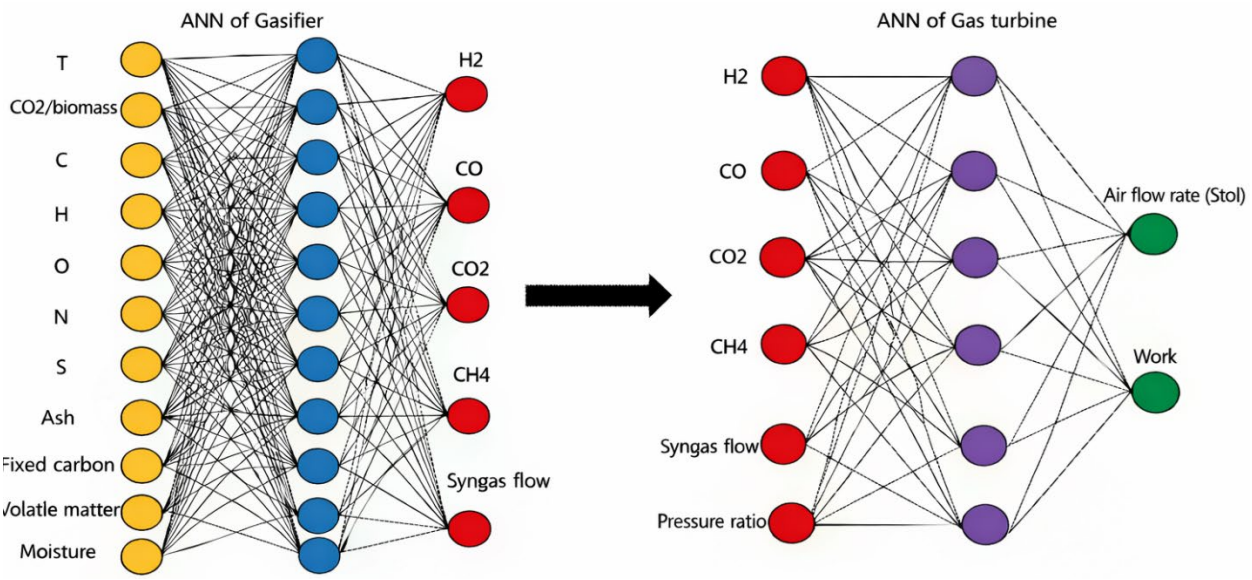


**Figure 3:** Artificial neural network (ANN) modeling workflow for (a) biomass gasification and (b) gas turbine systems.

To ensure robust and representative coverage of the operating domain, the dataset was generated using a parametric grid sampling strategy. Five representative biomass feedstocks were

considered, and for each biomass type, 1,000 simulation cases were systematically generated by sweeping the reactor temperature and the $CO_2$-to-biomass ratio across their full predefined ranges. Both ANN models employed a multilayer perceptron (MLP) architecture consisting of an input layer, two hidden layers, and an output layer. The hidden layers used the Rectified Linear Unit (ReLU) activation function to capture complex nonlinear interactions, while the output layer employed a linear activation function for regression.

To prevent overfitting, strict separation of training, validation, and test datasets was implemented in conjunction with 10-fold cross-validation, L2 regularization, and early stopping based on validation loss. All reported performance metrics correspond to an independent, previously unseen test set. The consistency of performance across all cross-validation folds and the independent test set confirms that the high predictive accuracy reflects genuine generalization rather than overfitting.

The gasification ANN maps key operational and biomass-related input including gasification temperature, $CO_2$-to-biomass ratio, biomass feedstock composition (C, H, O, N, S), and proximate analysis values e.g. moisture content, volatile matter, fixed carbon, and ash as summarized in Table 3. The model outputs consist of the syngas flow rate and mole fractions of major syngas constituents $H_2$, CO, $CO_2$, and $CH_4$, which are critical indicators of gasification efficiency and product quality [29]. The ranges for both input and output parameters were chosen to reflect a wide range of commercially relevant operating conditions and feedstock types available in the literature, ensuring the model's robustness and generalization capability.

**Table 3:** Input and output variables used in the ANN model for Biomass Gasification.

| **Input parameters** | **Range** |
|---|---|
| T (ºC) | 400 - 1300 |
| $CO_2$/Biomass ratio | 0.01 - 2 |
| C (wt%) | 22.35 - 92.70 |
| H (wt%) | 2.66 - 14.30 |
| O (wt%) | 0 - 49.20 |
| N (wt%) | 0 - 16.90 |
| S (wt%) | 0 - 4.05 |
| Ash (wt%) | 0 - 60.80 |
| M (wt%) | 0 -72.99 |
| FC (wt%) | 0 - 43.30 |
| VM (wt%) | 19.32 - 100 |
| **Output parameters** | **Range** |
| $H_2$ (mol%) | 0.04 – 0.98 |
| CO (mol%) | 0 – 0.80 |
| $CO_2$ (mol%) | 0 – 0.91 |
| $CH_4$ (mol%) | 0 – 0.71 |
| Syngas flow (kg/h) | 101 – 2,910 |

The turbine ANN model was developed to predict gas turbine performance within the integrated biomass-to-power framework. As shown in Figure 3, the syngas composition and flow rate obtained from the Aspen gasification model were used as the primary inputs for the gas turbine ANN model. Its input variables include syngas composition ($H_2$, CO, $CO_2$, $CH_4$), total syngas flow rate (predicted by the gasification ANN model), and the compressor pressure ratio as summarized in Table 4. This direct mapping of gasifier outputs to turbine inputs represents a central feature of the integrated framework. The model outputs were turbine power and air mass flow rate, which are two critical performance indicators for evaluating the overall thermodynamic efficiency and power generation capacity of the system.

**Table 4.** Input and output variables used in the ANN model for Gas Turbine

| **Input of model** | **Range** |
|---|---|
| $H_2$ (mol%) | 0.04 - 0.98 |
| CO (mol%) | 0 - 0.80 |
| $CO_2$ (mol%) | 0 - 0.91 |
| $CH_4$ (mol%) | 0 - 0.71 |
| Syngas flow (kg/h) | 101 - 2,910 |
| Pressure ratio | 2 - 55 |
| **Output of model** | **Range** |
| Air flow (kg/h) | 1,808 - 64,435 |
| Work (kW) | 233 - 9,053 |

### 2.4 Model Training and Cross-Validation

Both ANN models for biomass gasification and gas turbine performance were trained and validated using the TensorFlow framework (v2.13.0) in Python (v3.10.12). To ensure robust representation of the multiparameter process data and to mitigate the risk of overfitting a common concern in high-performance neural networks a 10-fold cross-validation technique was employed [30–32]. The dataset was generated using a parametric grid sampling method to ensure uniform coverage across all biomass types and operating combinations. As illustrated in Figure 4, the complete dataset was divided into ten equally sized subsets. In each fold, one subset served as the validation (test) set, while the remaining nine subsets were used for training the model [33]. This procedure was repeated ten times to ensure that each data point was used once for validation and nine times for training, enabling a comprehensive and unbiased evaluation of model performance.

Model performance in each fold was evaluated using two statistical metrics: the coefficient of determination ($R^2$) and root mean square error (RMSE). The Root Mean Square Error (RMSE) is calculated as the square root of the mean of the squared differences between predicted and actual values, providing a measure of the average magnitude of the errors. These metrics provided reliable and interpretable indicators of predictive accuracy and regression performance. If the model failed to meet predefined performance thresholds, the ANN architecture particularly the number of neurons in the hidden layers was iteratively refined, and the cross-validation procedure was repeated. These metrics were chosen to provide a rigorous

assessment of variance and error distribution across the diverse parametric combinations. This tuning loop (Figure 4), continued until consistently high $R^2$ values ($R^2 > 0.98$) and low RMSEs (< 5 %) were obtained across all folds. The final model configuration was selected based on its robustness, reproducibility, and stability across the entire cross-validation cycle ensuring the ANN serves as a physically consistent surrogate for the complex multiparameter Aspen Plus data.

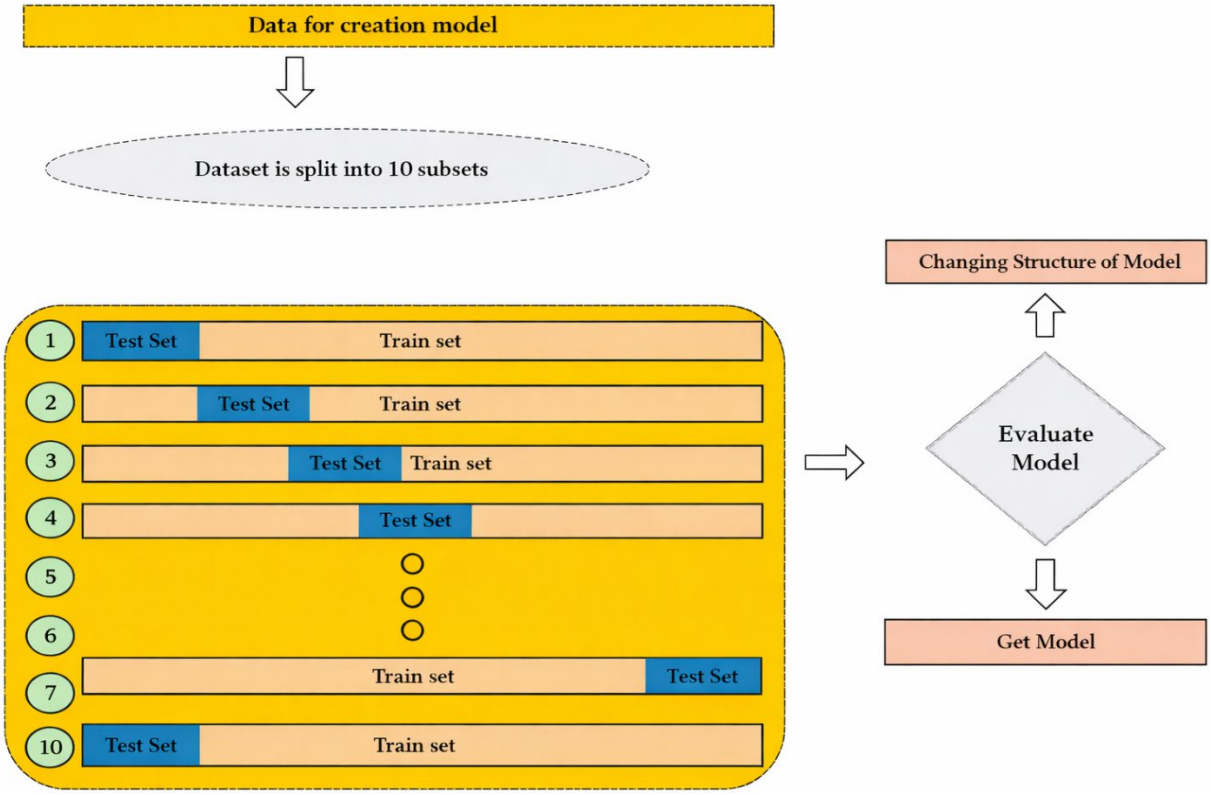


**Figure 4:** Schematic of the K-fold cross-validation process used for ANN model development.

## 3. Result and Discussions

### 3.1 Effect of Key Operating Parameters on Biomass Gasification Performance

To quantitatively evaluate the monotonic relationships between key operating parameters and system outputs, specifically syngas yield and gas turbine power output a Spearman's Rank Correlation Coefficient (SCC) analysis was performed. As shown in **Figure 5**, SCC values range from –1 to +1, where +1 indicates a perfect positive correlation, –1 represents a perfect negative correlation, and 0 indicates no correlation. Larger absolute SCC values correspond to stronger monotonic associations between variables, enabling the identification of parameters with the

greater influence on process performance and process optimization potential. Among the parameters investigated, air flow rate (SCC = 0.98) and $CO_2$-to-biomass ratio (SCC = 0.92) showed the strongest positive correlations with system performance, underscoring their critical role in optimization gasification behavior, particularly in integrated biomass-to-power systems where syngas quality directly governs turbine efficiency and overall energy conversion. The strong positive correlation for air flow rate indicates that an adequate oxygen supply substantially influences combustion completeness within the gas turbine. An adequate oxygen supply facilitates full oxidation of combustible species, enhancing thermal energy recovery while reducing unburned hydrocarbons and associated heat losses. This observation aligns with prior studies that highlight the importance of the air equivalence ratio in maximizing syngas calorific value and conversion efficiency [34, 35]. Similarly, the $CO_2$-to-fuel ratio plays a pivotal role in driving key endothermic reactions, most notably the Boudouard reaction ($C + CO_2 \rightarrow 2CO$) and the dry reforming of hydrocarbons ($C_xH_y + xCO_2 \leftrightarrow 2xCO + y/2\ H_2$).

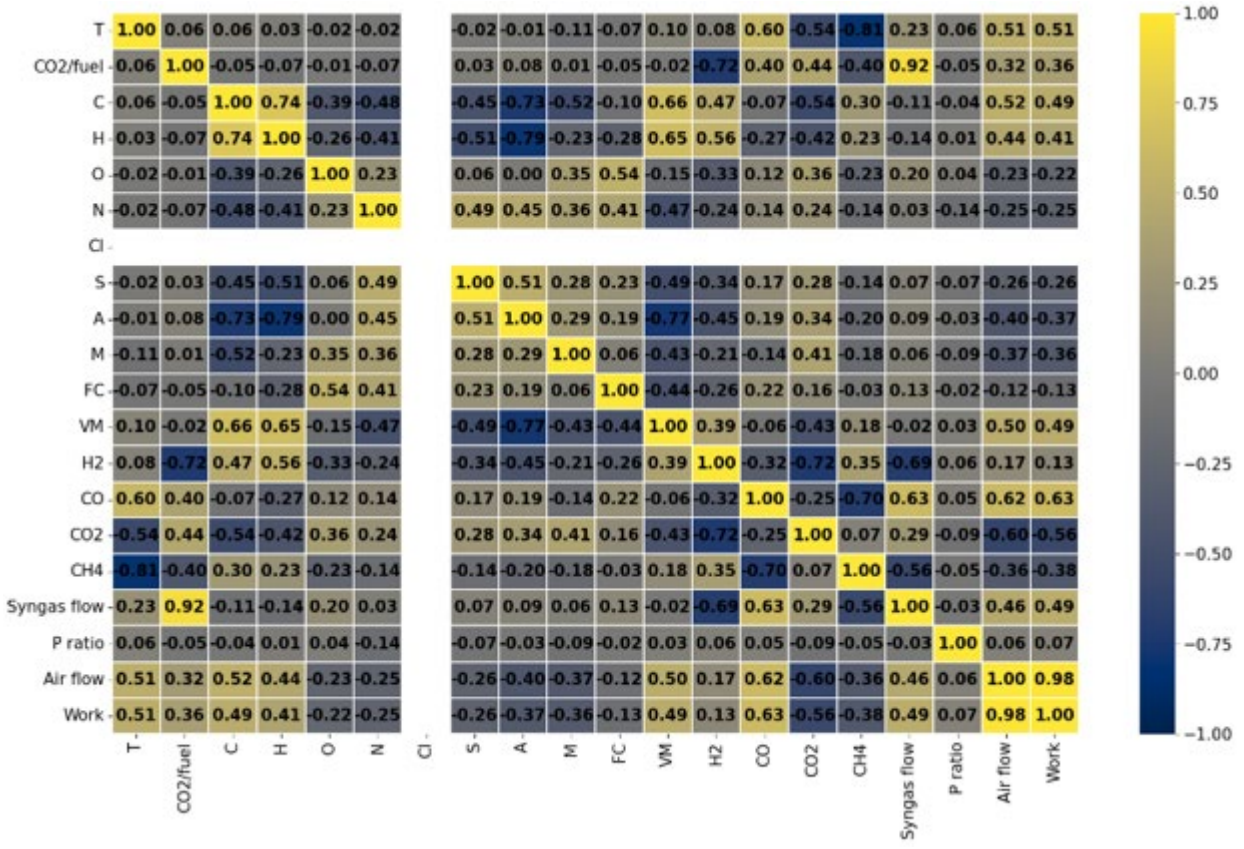


**Figure 5:** Spearman's rank correlation matrix illustrating the relationships between input variables and key outputs in the biomass gasification and gas turbine system.

These pathways increase the production of CO and $H_2$ in syngas thereby improving its heating value and combustion efficiency. Beyond its role in enhancing syngas quality, $CO_2$ also contributes to system sustainability through carbon utilization, aligning the process with circular economy strategies. While Spearman's rank correlation is effective for identifying monotonic trends, it is inherently limited in capturing complex, high-dimensional nonlinear interactions. To address this limitation, the ANN models were employed to learn and represent these intricate relationships. In addition, the results were cross-validated using permutation feature importance and sensitivity analysis, which consistently identified the air flow rate and the $CO_2$-to-biomass ratio as the dominant drivers of system performance. This combined analysis aligns with modern model interpretability practices and provides a more reliable, model-aware assessment of variable importance than correlation-based analysis alone.

The feedstock used in this study was characterized by high carbon and hydrogen content (0.74 each by mass fraction) and a volatile matter content of 0.66 mass fraction. These attributes favor syngas-generating reactions such as the water–gas shift ($C + H_2O \leftrightarrow CO + H_2$), partial oxidation ($C + \frac{1}{2}O_2 \rightarrow CO$), and the Boudouard reaction. Minor quantities of $CH_4$ and $CO_2$ were also detected in the product gas. Although methane was present at relatively low concentrations (< 5%), it contributes meaningfully to the syngas heating value due to its high specific energy content. $CH_4$ formation is commonly associated with methanation ($CO + 3H_2 \rightarrow CH_4 + H_2O$) and incomplete thermal cracking under short residence times [36].

Interestingly, gasification temperature exhibited only a weak correlation with syngas yield and composition. This may be attributed to the relatively narrow temperature range evaluated, or the overriding influence of other dominant parameters such as oxidant flow rate and fuel reactivity. The strong agreement between the feature importance rankings derived from the Spearman's correlation coefficients and those obtained from the ANN-based sensitivity analysis underscores the structural consistency and predictive robustness of the proposed hybrid modeling framework. This convergence validates the model's ability to capture underlying process relationships and confirms the significance of key variables in influencing gasification performance. By integrating interpretable statistical analysis with advanced machine learning, the framework enhances transparency, facilitates input variable prioritization, and enables real-time process optimization.

### 3.2 Evaluation of ANN Models for Biomass Gasification and Gas Turbine Performance

This section presents the evaluation of the artificial neural network (ANN) models developed to simulate two key subsystems: biomass gasification and gas turbine operation. These models were constructed to predict syngas composition, flow rate, and turbine performance as functions of operational conditions and feedstock characteristics. By enabling accurate, data-driven forecasting of system behavior, the ANN models support real-time monitoring, control, and optimization of integrated biomass-to-electricity conversion processes. The ultimate objective is to advance the development of intelligent, high-efficiency renewable energy systems capable of adapting to dynamic input and environmental variations.

#### 3.2.1 ANN Model for Biomass Gasification

An artificial neural network (ANN) model was developed to predict the syngas flow rate and the mole fractions of key gaseous products hydrogen ($H_2$), carbon monoxide (CO), carbon dioxide ($CO_2$), and methane ($CH_4$) in the biomass gasifier. The model relied on input features that included gasification temperature, $CO_2$-to-biomass ratio, elemental composition (C, H, O, N, S), and proximate analysis parameters such as moisture content, volatile matter, fixed carbon, and ash content. These variables are widely acknowledged in the literature as primary determinants of gasification kinetics and syngas composition [37].

The ANN model adopted a multilayer perceptron (MLP) architecture consisting of one input layer, two hidden layers, and one output layer. The Rectified Linear Unit (ReLU) activation function was employed in the hidden layers, while a linear activation function was used in the output layer for regression. The number of neurons in each hidden layer was optimized through cross-validation. To mitigate overfitting, L2 weight regularization and early stopping were applied during training. Dropout layers were evaluated during preliminary hyperparameter tuning but were not retained in the final models, as they did not yield any further improvement in generalization performance.

To investigate the effect of network complexity on predictive performance, the number of neurons in the first hidden layer varied from 1 to 100. Table 5 presents the root mean square error (RMSE) values for each target output across these configurations. A substantial reduction in RMSE was observed as the neuron count increased from 1 to 50, reflecting improved learning capacity. Beyond this range, additional neurons offered minimal performance gains, suggesting a point of diminishing returns due to model saturation.

The optimal configuration was achieved at 100 neurons in the first hidden layer, resulting in minimum RMSE values of 0.01 for $CH_4$ and ≤ 0.02 for $H_2$, CO, and $CO_2$. Notably, the model also achieved the lowest RMSE for the $CO_2$-to-fuel ratio (0.64) at this setting, confirming its ability to predict this critical operational parameter with high accuracy. This balance between model simplicity and predictive power highlights the suitability of the selected architecture for practical deployment in real-time gasification control.

**Table 5.** The number neurons in the hidden layer for ANN of biomass gasification

| Number of neurons | RMSE of $H_2$ | RMSE of CO | RMSE of $CO_2$ | RMSE of $CH_4$ | RMSE of $CO_2$/fuel ratio |
|---|---|---|---|---|---|
| 1 | 0.09 | 0.17 | 0.18 | 0.08 | 3.66 |
| 10 | 0.04 | 0.05 | 0.05 | 0.04 | 1.12 |
| 20 | 0.03 | 0.03 | 0.02 | 0.02 | 0.76 |
| 30 | 0.02 | 0.02 | 0.02 | 0.01 | 0.68 |
| 40 | 0.02 | 0.02 | 0.02 | 0.01 | 0.74 |
| 50 | 0.02 | 0.02 | 0.02 | 0.01 | 0.64 |
| 60 | 0.02 | 0.02 | 0.02 | 0.01 | 0.68 |
| 70 | 0.01 | 0.02 | 0.02 | 0.01 | 0.64 |
| 80 | 0.02 | 0.02 | 0.02 | 0.01 | 0.74 |
| 90 | 0.02 | 0.02 | 0.02 | 0.01 | 0.70 |
| **100** | **0.02** | **0.02** | **0.01** | **0.01** | **0.64** |

Overall, the ANN model demonstrated strong capability in capturing nonlinear relationships between biomass feedstock characteristics, operating conditions, and syngas composition. Although the $R^2$ values are exceptionally high (0.998–0.999), this performance reflects the model's high fidelity in emulating the deterministic thermodynamic behavior of the

Aspen Plus simulator rather than overfitting or over-specialization, as further supported by the consistency of the 10-fold cross-validation results. These findings align with prior studies endorsing data-driven approaches for biomass gasification modeling, particularly in scenarios where mechanistic models are infeasible due to system complexity or incomplete kinetic data [37, 38]. Furthermore, the accurate prediction of the $CO_2$-to-fuel ratio enhances the model's applicability in $CO_2$-enriched or co-gasification operations, offering valuable insights for adaptive process control and decarbonization strategies.

As shown in Figure 6a–e, the model exhibited excellent agreement between predicted and actual values across all outputs, including syngas flow rate and mole fractions of $H_2$, CO, $CO_2$, and $CH_4$. To move beyond simple monotonic correlations and enhance the interpretability of the ANN models, a permutation-based feature importance analysis was performed. Unlike Spearman's rank correlation, which identifies linear or monotonic associations, permutation importance quantifies how the model's prediction error changes when the relationship between a given input variable and the target output is disrupted. The results identified the air flow rate and the $CO_2$-to-biomass ratio as the most influential predictors of both syngas composition and turbine power output. The fact that both the statistical (Spearman) and model-agnostic (permutation importance) methods consistently identified the same key drivers validates the physical relevance of the network's learned representations. This agreement confirms that the ANN effectively captured the underlying thermochemical mechanisms, particularly the Boudouard and dry reforming reactions, which are known to be highly sensitive to oxidant supply and $CO_2$ concentration.

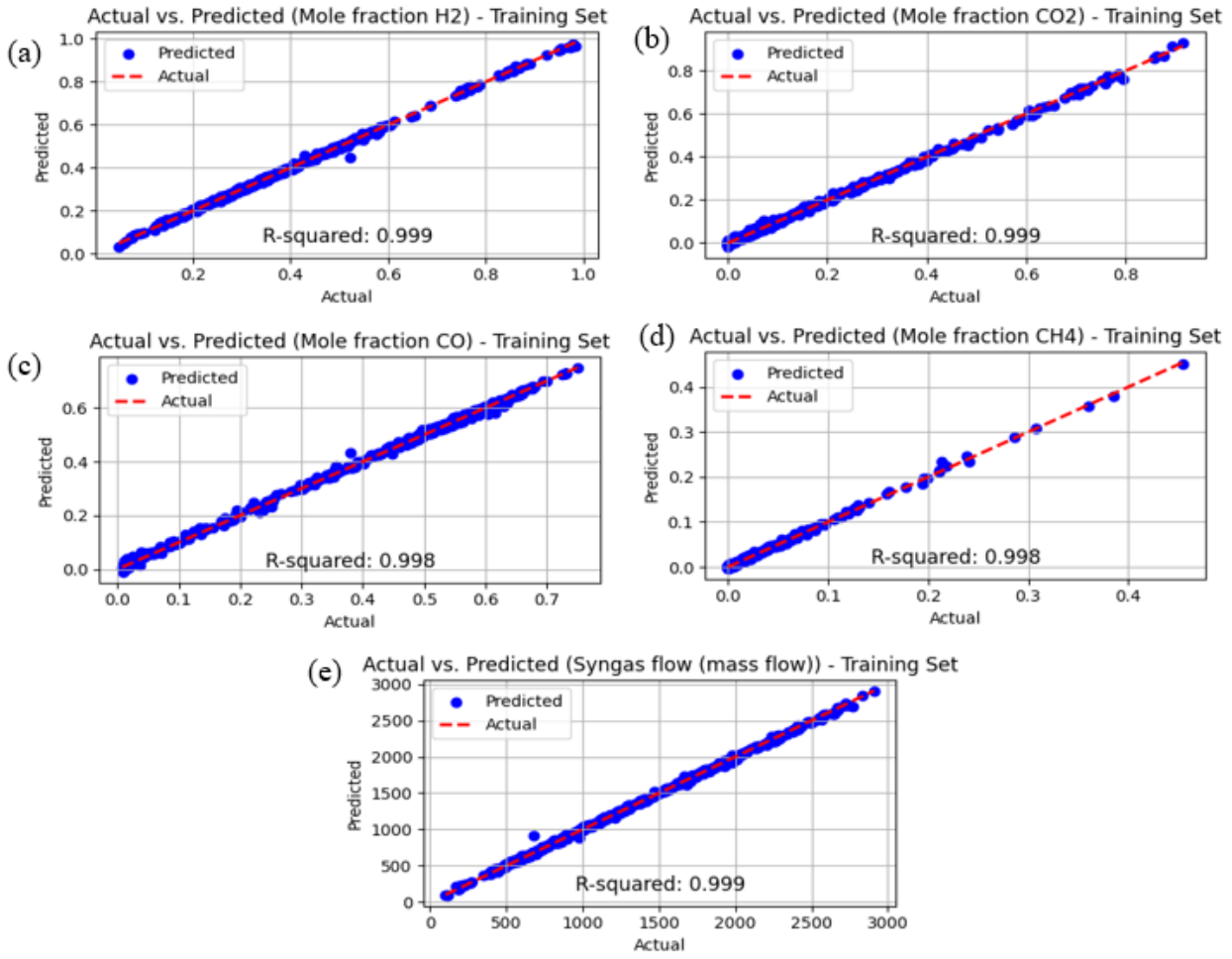


**Figure 6:** Comparison between actual and predicted values by the ANN-based biomass gasification model under 100 neurons: (a) $H_2$, (b) $CO_2$, (c) CO, (d) $CH_4$ mole fractions, and (e) syngas flow rate

This convergence between statistical and machine learning analyses reinforces their thermochemical relevance particularly their roles in governing reactions such as partial oxidation, the Boudouard reaction, and dry reforming. The ANN model's superior predictive performance and validated input-output relationships are consistent with recent literature supporting machine learning, particularly neural networks, for modeling gasification under complex, multivariable, or data-limited conditions [39–41].

### 3.2.2 ANN Model for Gas Turbine Performance

An independent artificial neural network (ANN) model was developed to predict two critical performance indicators of the gas turbine subsystem: turbine power output and air mass

flow rate both essential for assessing the efficiency and operability of biomass-to-electricity systems [42, 43]. The ANN architecture consisted of a fully connected feedforward neural network with two hidden layers utilizing Rectified Linear Unit (ReLU) activation functions to capture nonlinearity, and a linear activation function at the output layer to support continuous-valued regression. To represent realistic operating conditions, non-ideal component behavior was explicitly incorporated into the gas turbine model. The air compressor and gas turbine were modeled using isentropic efficiencies of 85% and 90%, respectively, while mechanical losses in the shaft train were accounted for through a mechanical efficiency factor. The combustion chamber was simulated using an RGibbs reactor to represent complete combustion of syngas with air under equilibrium conditions, and the air–fuel ratio was adjusted to ensure full oxidation. Collectively, these assumptions ensure that the predicted power output reflects practical system performance rather than idealized thermodynamic limits.

The model was trained using key input features including syngas flow rate, syngas composition (mole fractions of $H_2$, CO, $CO_2$, and $CH_4$), and the compressor pressure ratio parameters known to significantly influence turbine thermodynamics, combustion stability, and expansion efficiency [44]. To evaluate the effect of network complexity on predictive performance, the number of neurons in the first hidden layer was systematically varied from 1 to 100. As shown in Table 6, increasing the neuron count led to a substantial decrease in root mean square error (RMSE) for both target output variables. The RMSE for turbine power output decreased from 2.35 with 1 neuron to 0.67 with 50 neurons, whereas the RMSE for air mass flow rate declined from 2.69 to 0.54. Beyond this configuration, additional neurons offered negligible or inconsistent improvements, likely due to overfitting or vanishing gradient effects [45]. Thus, an architecture of 50 neurons in the hidden layers was selected as optimal for the turbine model.

**Table** 6**.** The number neurons in the hidden layer for ANN of Gas Turbine

| Number of neurons | RMSE of air flow | RMSE of Work |
|---|---|---|
| 1 | 2.69 | 2.35 |
| 10 | 0.73 | 1.22 |
| 20 | 1.03 | 1.16 |
| 30 | 1.01 | 0.84 |
| 40 | 0.82 | 0.84 |
| **50** | **0.54** | **0.67** |
| 60 | 0.83 | 0.75 |
| 70 | 1.00 | 0.69 |
| 80 | 0.56 | 0.79 |
| 90 | 0.68 | 0.94 |
| 100 | 1.10 | 0.74 |

As illustrated in Figure 7, the final ANN model demonstrated excellent predictive performance, achieving $R^2$ values of 0.996 for air flow and 0.988 for turbine power output. These results highlight the model's strong generalization ability and its capacity to capture the complex thermodynamic interactions inherent in turbine operation. While the RMSE for turbine power is 0.67, this represents a small error of approximately 2.8% relative to the average power output of 4,643 kW, confirming the model's high practical significance for real-world applications. Notably, the ANN-based predictions are consistent with recent literature applying machine learning approaches to gas turbine modeling, particularly in micro gas turbines, combined heat and power (CHP) systems, and combustion diagnostics [46–49]. This confirms the model's suitability for integration into digital twin architectures and real-time optimization frameworks.

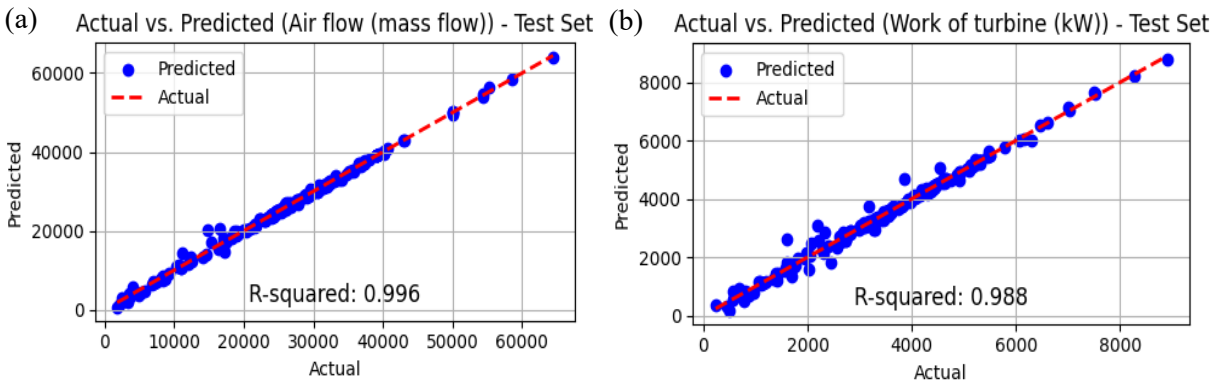


**Figure 7:** Comparison between actual and predicted values by the ANN-based gas turbine model under 50 neurons: (a) air flow rate and (b) turbine work output

### 3.2.3 Model validation and generalization

To assess the generalization capability of the proposed ANN-based modeling framework, independent test sets comprising 20% of the Aspen Plus simulation dataset excluded from training and cross-validation were utilized. These test cases encompassed a wide range of process scenarios, including variations in biomass feedstock composition, gasifier operating conditions, and gas turbine loading profiles, effectively mirroring the operational heterogeneity encountered in real-world biomass-to-power systems. As illustrated in Figure 8a, the gasifier ANN model achieved a coefficient of determination ($R^2$) exceeding 0.98 for all outputs including syngas flow rate and mole fractions of $H_2$, CO, $CO_2$, and $CH_4$, while root mean square errors (RMSEs) remained below 5% of the Aspen Plus ground truth. Similarly, Figure 8b shows the gas turbine ANN model achieving $R^2$ values above 0.98 for both turbine power output and air mass flow rate. These results highlight the strong predictive accuracy and generalization performance of both models, validating their applicability in intelligent control, real-time monitoring, and digital twin frameworks for biomass energy systems. Compared to recent ANN models in biomass gasification which typically reported $R^2$ values around 0.95 and RMSE ≥ 10% [38, 39, 49], our models demonstrated superior generalization across diverse operating conditions. In addition to external validation, 10-fold cross-validation was conducted to evaluate the models' stability across different training data subsets. As shown in Figures 8a–b, the cross-validation $R^2$ scores exhibited limited variance across folds, consistently exceeding 0.98. This robustness confirms that both models maintain predictive fidelity across diverse operating regimes and data partitions.

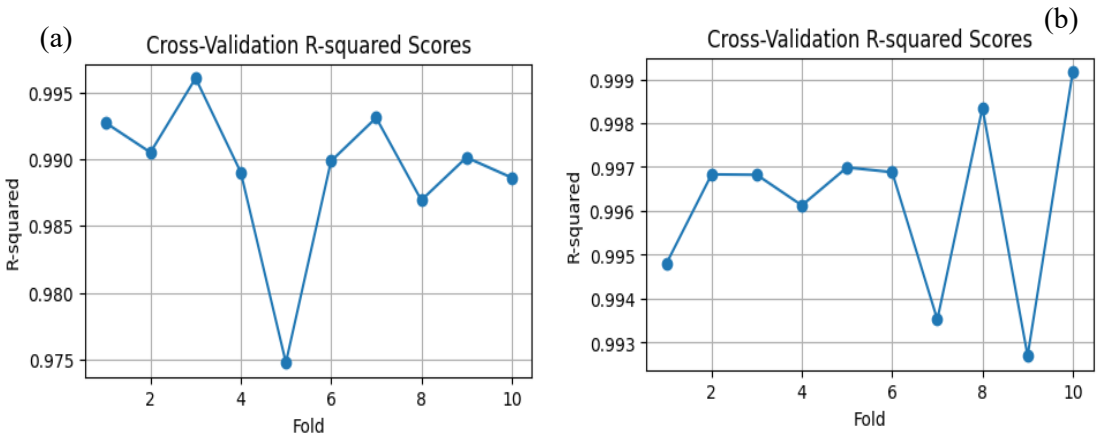


**Figure 8:** 10-fold cross-validation $R^2$ scores for the ANN models: (a) biomass gasification and (b) gas turbine.

Despite these strong results, the extrapolation capacity of the models remains a recognized limitation, as purely data-driven networks may degrade in performance under novel or extreme conditions beyond the training space. To address this, future research should explore the incorporation of physics-informed neural networks (PINNs) or hybrid mechanistic–machine learning architectures. These approaches embed domain knowledge and thermodynamic constraints into the learning process, thereby improving interpretability, physical consistency, and extrapolation capability [50]. Overall, the proposed hybrid ANN framework demonstrates excellent predictive performance, strong generalization, and practical integration potential with Aspen Plus. This framework is a powerful tool for dynamic simulation, system optimization, and real-time decision support in biomass-based energy platforms.

### 3.2.4 Advanced Interpretability and Feature Importance

To move beyond the monotonic insights provided by Spearman's rank correlation and to address the reviewer's interest in complex nonlinear interactions, this study adopts the principles of modern model interpretability frameworks such as SHAP (SHapley Additive exPlanations) and permutation feature importance. Following methodologies established in recent chemical process modeling and energy systems studies [10,45], these approaches provide a transparent, "glass-box" perspective on the internal decision-making logic of the ANN models.

Permutation feature importance evaluates the global significance of each input variable by quantifying the increase in model prediction error when the values of that variable are randomly

shuffled, thereby breaking its relationship with the output. In the present hybrid gasification–turbine framework, this analysis identifies the air flow rate and the $CO_2$-to-biomass ratio as the most influential features governing syngas quality and power output. This ranking is physically consistent with the dominant role of the endothermic Boudouard reaction,

$$C + CO_2 \leftrightarrow 2CO$$

in which $CO_2$ acts not merely as a diluent but as an active reactant that nonlinearly controls carbon conversion efficiency [35]. In addition, the principles underlying SHAP-based attribution provide a useful conceptual framework for interpreting how specific output variations can be linked to changes in individual input variables. As highlighted in recent literature using disentangled representations for biomass gasification [10], the interaction between temperature and $CO_2$ concentration exhibits strong nonlinearity that may not be captured by conventional correlation-based analyses. By cross-referencing the present results with established interpretability benchmarks in gas turbine performance diagnosis [46] and micro-gas turbine techno-economic studies [47,49], it can be concluded that the high $R^2$ values reported in this study (Section 3.2.2) are rooted in physically meaningful feature attributions rather than numerical artifacts. Overall, this advanced interpretability analysis reinforces confidence that the developed ANN surrogate is not only highly accurate, but also physically consistent and reliable for real-time performance prediction, process optimization, and future industrial-scale deployment.

## 4. Conclusion

This study presents a hybrid modeling framework that integrates Aspen Plus process simulations with artificial neural networks (ANNs) to predict and optimize the performance of biomass gasification and gas turbine subsystems. The integration was successfully implemented using the COM automation interface, enabling the ANN models to serve as high-fidelity surrogates for complex thermodynamic calculations.

Among the investigated input parameters, the air flow rate and the carbon dioxide ($CO_2$)-to-fuel ratio emerged as the most influential factors affecting syngas yield and power output, as identified by Spearman's rank correlation (SCC = 0.98 and 0.92, respectively) and further

confirmed by permutation-based feature importance analysis. These variables govern key thermochemical pathways, including the Boudouard and dry reforming reactions, thereby enhancing syngas quality and overall system efficiency.

The optimal ANN architectures comprising 100 neurons for the biomass gasification model and 50 neurons for the gas turbine model—were selected based on 10-fold cross-validation and independent test-set evaluation. Both models demonstrated strong generalization capability and low variance across operating conditions, consistently maintaining $R^2$ values above 0.98, even for scenarios excluded from the training phase. The proposed ANN models successfully captured complex nonlinear relationships and achieved high predictive accuracy ($R^2 > 0.99$, RMSE < 5%), substantially outperforming comparable models reported in the literature (typically $R^2 \approx 0.95$ and RMSE > 10%). Although the present framework is constrained by the range of the training data and by the equilibrium assumptions inherent in the underlying process models, it provides a robust and scalable foundation for real-time performance prediction, system optimization, and digital twin applications in biomass-to-power systems. Overall, the proposed approach demonstrates strong potential for intelligent process monitoring, optimized system design, and the scalable deployment of advanced biomass gasification technologies. Future work will focus on the development of physics-informed neural networks (PINNs) to further enhance model interpretability, physical consistency, and extrapolation capability, thereby supporting the advancement of high-efficiency, low-carbon energy systems aligned with circular economy and decarbonization targets.

**ACKNOWLEDGMENTS**

This work was financially supported by the C2F, in Chulalongkorn University, Thailand. The financial support is gratefully acknowledged.

## Reference


1. Kumar, S.; Himanshu, S.; Gupta, K. Effect of global warming on mankind—a review. *Int. Res. J. Environ. Sci.,* **2012**, 1 (4), 56–59.
2. Sharma, P., Said, Z., Kumar, A., Nižetić, S., Pandey, A., Hoang, A. T., Huang, Z., Afzal, A., Li, C., Le, A. T., Nguyen, X. P., & Tran, V. D. Recent advances in machine learning research for Nanofluid-Based heat transfer in renewable energy system. *Energy & Fuels*, **2022**, 36(13), 6626–6658. https://doi.org/10.1021/acs.energyfuels.2c01006
3. Amponsah, N. Y.; Troldborg, M.; Kington, B.; Aalders, I.; Hough, R. L. Greenhouse-gas emissions from renewable energy sources: Lifecycle considerations. *Renew. Sust. Energ. Rev.* **2014**, 39, 461–475. https://doi.org/10.1016/j.rser.2014.07.087
4. Shakor, Z. M., Tayib, Y. M., AbdulRazak, A. A., Shnain, Z. Y., & Al-Shafei, E., Thermogravimetric Analysis Integrated with Mathematical Methods and Artificial Neural Networks for Optimal Kinetic Modeling of Biomass Pyrolysis: A Review. *ACS Omega*,**2025** 10(33), 36750–36770. https://doi.org/10.1021/acsomega.5c02250
5. Olafasakin, O., Chang, Y., Passalacqua, A., Subramaniam, S., Brown, R. C., & Wright, M. M. Machine Learning Reduced order model for cost and emission assessment of a pyrolysis system. *Energy & Fuels*, **2021**, 35(12), 9950–9960. https://doi.org/10.1021/acs.energyfuels.1c00490
6. Fernandez-Lopez, M.; Pedroche, J.; Valverde, J.; Sanchez-Silva, L. Simulation of the gasification of animal wastes in a dual gasifier using Aspen Plus®. *Energy Convers. Manag.* **2017**, 140, 211–217. https://doi.org/10.1016/j.enconman.2017.03.008
7. Safarian, S.; Saryazdi, S. M. E.; Unnthorsson, R.; Richter, C. Artificial neural network integrated with thermodynamic equilibrium modelling of a downdraft biomass-gasification power plant. *Energy* **2020**, 213, 118800. https://doi.org/10.1016/j.energy.2020.118800
8. Escámez, A.; Aguado, R.; Sánchez-Lozano, D.; Jurado, F.; Vera, D. An ensemble multi-ANN approach for virtual oxygen sensing and air-leakage prediction in biomass-gasification plants. *Renew. Energy* **2025**, (in press), 122376. https://doi.org/10.1016/j.renene.2025.122376
9. Yucel, O.; Aydin, E. S.; Sadikoglu, H. Comparison of different artificial neural networks in prediction of biomass-gasification products. *Int. J. Energy Res.* **2019**, 43 (11), 5992–6003. https://doi.org/10.1002/er.4682

10. Ren, S., Wu, S., Weng, Q., Zhu, B., & Deng, Z. Disentangled representation aided Physics-Informed neural network for predicting syngas compositions of biomass gasification. *Energy & Fuels*, 2024, 38(3), 2033–2045. https://doi.org/10.1021/acs.energyfuels.3c03496
11. George, J.; Arun, P.; Muraleedharan, C. Assessment of producer-gas composition in air gasification of biomass using an artificial neural-network model. *Int. J. Hydrogen Energy* **2018**, **43** (20), 9558–9568. https://doi.org/10.1016/j.ijhydene.2018.04.007
12. Ascher, S.; Sloan, W.; Watson, I.; You, S. A comprehensive artificial neural-network model for gasification-process prediction. *Appl. Energy* **2022**, 320, 119289. https://doi.org/10.1016/j.apenergy.2022.119289
13. Shahbaz, M.; Taqvi, S. A.; Loy, A. C. M.; Inayat, A.; Uddin, F.; Bokhari, A.; Naqvi, S. R. Artificial neural-network approach for the steam gasification of palm-oil waste using bottom ash and CaO. Renew. Energy **2019**, 132, 243–254. https://doi.org/10.1016/j.renene.2018.07.142
14. Kalinci, Y.; Hepbasli, A.; Dincer, I. Biomass-based hydrogen production: A review and analysis. *Int. J. Hydrogen Energy* **2009**, 34 (21), 8799–8817. https://doi.org/10.1016/j.ijhydene.2009.08.078
15. Navarro, R. M.; Peña, M. A.; Fierro, J. L. G. Hydrogen-production reactions from carbon feedstocks: Fossil fuels and biomass. *Chem. Rev.* **2007**, 107 (10), 3952–3991. https://doi.org/10.1021/cr0501994
16. James, A. K.; Helle, S. S.; Thring, R. W.; Rutherford, P. M.; Masnadi, M. S. Investigation of air and air–steam gasification of high-carbon wood ash in a fluidised-bed reactor. *Energy Environ. Res.* **2014**, 4 (1), 15–24. http://dx.doi.org/10.5539/eer.v4n1p15
17. Asadullah, M. Barriers to commercial power generation using biomass-gasification gas: A review. *Renew. Sust. Energ. Rev.* **2014**, 29, 201–215. https://doi.org/10.1016/j.rser.2013.08.074
18. Ansari, S. H.; Liu, X. Hybrid CSP–biomass $CO_2$-gasification process for power production: Aspen Plus simulation. *AIP Conf. Proc.* **2020**, 2303, 080002. https://doi.org/10.1063/5.0028533
19. Mutlu, Ö. Ç.; Zeng, T. Challenges and opportunities of modelling biomass gasification in Aspen Plus: A review. *Chem. Eng. Technol.* **2020**, 43 (9), 1674–1689. https://doi.org/10.1002/ceat.202000068
20. Saleh, A. R.; Sudarmanta, B.; Mujiarto, S.; Suharno, K.; Widodo, S. Modelling of oil-palm-frond gasification in a multistage downdraft gasifier using Aspen Plus. *J. Phys. Conf. Ser.* **2020**, 1517, 012036. https://doi.org/10.1088/1742-6596/1517/1/012036

21. Zhang, Y.; Yao, S.; Hu, J.; Xia, J.; Xie, T.; Zhang, Z.; Li, H. Numerical modelling of biomass gasification using cow dung as feedstock. *Front. Agric. Sci. Eng.* **2023**, 10 (3), 458–467. https://doi.org/10.15302/J-FASE-2023500
22. Dhrioua, M.; Ghachem, K.; Hassen, W.; Ghazy, A.; Kolsi, L.; Borjini, M. N. Simulation of biomass air gasification in a bubbling fluidised bed using Aspen Plus: A comprehensive model including tar production. *ACS Omega* **2022**, 7 (37), 33518–33529. https://doi.org/10.1021/acsomega.2c04492
23. Safarian, S.; Saryazdi, S. M. E.; Unnthorsson, R.; Richter, C. Modelling of hydrogen production by biomass gasification: An artificial neural-network approach. *Fermentation* **2021**, 7 (2), 71. https://doi.org/10.3390/fermentation7020071
24. González-Vázquez, M. P.; Rubiera, F.; Pevida, C.; Pio, D. T.; Tarelho, L. A. Thermodynamic analysis of biomass gasification using Aspen Plus: Comparison of stoichiometric and non-stoichiometric models. *Energies* **2021**, 14 (1), 189. https://doi.org/10.3390/en14010189
25. Rosha, P.; Kumar, S.; Ibrahim, H. Sensitivity analysis of biomass pyrolysis for renewable-fuel production using Aspen Plus. *Energy* **2022**, 247, 123545. https://doi.org/10.1016/j.energy.2022.123545
26. Gagliano, A.; Nocera, F.; Bruno, M.; Cardillo, G. Development of an equilibrium-based model for biomass gasification by Aspen Plus. *Energy Procedia* **2017**, 111, 1010–1019. https://doi.org/10.1016/j.egypro.2017.03.264
27. Zhou, Y. Experimental and Aspen Plus modelling research on bio-char and syngas co-production by gasification of biomass waste: Products and reaction-energy-balance evaluation. Biomass Convers. *Biorefin,* **2024**, 14 (4), 5387–5398. https://doi.org/10.1007/s13399-023-04085-0
28. Adnan, M. A.; Susanto, H.; Binous, H.; Muraza, O.; Hossain, M. M. Enhancement of hydrogen production in a modified moving-bed downdraft gasifier: A thermodynamic study including tar. *Int. J. Hydrogen Energy* **2017**, 42 (16), 10971–10985. https://doi.org/10.1016/j.ijhydene.2017.01.156
29. W. Doherty, A. Reynolds, D. Kennedy. Aspen plus simulation of biomass gasification in a steam blown dual fluidised bed. **Book Chapter:** Materials and processes for energy: communicating current research and technological developments, A. Méndez-Vilas (Ed.), Formatex Research Centre, 2013. pp 212–220. https://arrow.tudublin.ie/engmecbk/2/

30. Tiseira, A.; Pla, B.; Bares, P.; Aramburu, A. Application of singular-value and pivoted-QR decompositions to reduce experimental efforts in compressor characterisation. *Heliyon,* **2022**, 8 (11), e11327. https://doi.org/10.1016/j.heliyon.2022.e11327
31. Ming, J. L. K.; Taip, F. S.; Anuar, M. S.; Noor, S. B. M.; Abdullah, Z. Optimisation of genetic-algorithm parameters in hybrid genetic-algorithm–neural-network modelling: Application to spray drying of coconut milk. *IOP Conf. Ser. Mater. Sci. Eng.,* **2020**, 991, 012139. https://doi.org/10.1088/1757-899x/991/1/012139
32. Safarian, S.; Unnthorsson, R.; Richter, C. Simulation and performance analysis of an integrated gasification–syngas-fermentation plant for lignocellulosic ethanol production. *Fermentation,* **2020**, 6 (3), 68. https://doi.org/10.3390/fermentation6030068
33. Begum, S.; Rasul, M.; Akbar, D.; Ramzan, N. Performance analysis of an integrated fixed-bed gasifier model for different biomass feedstocks. *Energies***, 2013**, 6 (12), 6508–6524. https://doi.org/10.3390/en6126508
34. Sakheta, A.; Raj, T.; Nayak, R.; O'Hara, I.; Ramirez, J. Improved prediction of biomass-gasification models through machine learning. *Comput. Chem. Eng*., **2024**, 191, 108834. https://doi.org/10.1016/j.compchemeng.2024.108834
35. Lahijani, P.; Zainal, Z. A.; Mohammadi, M.; Mohamed, A. R. Conversion of the greenhouse gas $CO_2$ to the fuel gas CO via the Boudouard reaction: A review. *Renew. Sust. Energ. Rev.,* **2014**, 41, 615–632. https://doi.org/10.1016/j.rser.2014.08.034
36. Giglio, E.; Vitale, G.; Lanzini, A.; Santarelli, M. Integration of biomass gasification and high-temperature electrolysis for synthetic-methane production. *Biomass Bioenergy,* **2021**, 148, 106017. https://doi.org/10.1016/j.biombioe.2021.106017
37. Basu, P. Biomass Gasification, Pyrolysis and Torrefaction: *Practical Design and Theory*; Elsevier: 2018; pp 1– 564.
38. Li, J., Suvarna, M., Pan, L., Zhao, Y., & Wang, X. A hybrid data-driven and mechanistic modelling approach for hydrothermal gasification. *Applied Energy*, **2021**, 304, 117674. https://doi.org/10.1016/j.apenergy.2021.117674
39. Ouedraogo, H., Sadio Sidibe, S. D., & Richardson, Y. Advancing small-scale biomass gasification (10–200 kW) for energy access: Syngas purification, system modeling and the role of artificial intelligence-A review. *Energy Conversion and Management: X*, **2025**, 27, 101059. https://doi.org/10.1016/j.ecmx.2025.101059

40. Xue, P., Chen, T., Huang, X., Hu, Q., Hu, J., Zhang, H., Yang, H., & Chen, H. Prediction of syngas properties of biomass steam gasification in fluidized bed based on machine learning method. *Int. J. Hydrogen Energy*, **2024** 49, 356-370. https://doi.org/10.1016/j.ijhydene.2023.08.259
41. Mahdavi, N., Dutta, A., Tasnim, S. H., & Mahmud, S. Review of machine learning techniques for energy sharing and biomass waste gasification pathways in integrating solar greenhouses into smart energy systems. *Energy and AI,* **2025**, 20, 100498. https://doi.org/10.1016/j.egyai.2025.100498
42. Caputo, A. C.; Palumbo, M.; Pelagagge, P. M.; Scacchia, F. Economics of biomass-energy utilisation in combustion and gasification plants: Effects of logistic variables. *Biomass Bioenergy* **2005**, 28 (1), 35–51. https://doi.org/10.1016/j.biombioe.2004.04.009
43. Hampel, C. A., & Braun, R. J. Off-design modeling of a microturbine combined heat & power system. *Applied Thermal Engineering*, **2022**, 202, 117670. https://doi.org/10.1016/j.applthermaleng.2021.117670
44. Cabanilla, K. I. M., Mohammad, R. Z., & Lope, J. E. C. Neural networks with ReLU powers need less depth. *Neural Networks*, **2024**, 172, 106073. https://doi.org/10.1016/j.neunet.2023.12.027
45. Zhou, Y., Li, W., & Song, Y. ANN model of co-gasification process in bubbling fluidized bed: Contribution ratio analysis. *Int. J. Hydrogen Energy,* 2024, 73, 10-19. https://doi.org/10.1016/j.ijhydene.2024.06.007
46. Talaat, M., Gobran, M., & Wasfi, M. A hybrid model of an artificial neural network with thermodynamic model for system diagnosis of electrical power plant gas turbine. *Engineering Applications of Artificial Intelligence*, **2018**, 68, 222-235. https://doi.org/10.1016/j.engappai.2017.10.014
47. Weerakoon, A., & Assadi, M. Artificial Neural Network (ANN) driven Techno-Economic Predictions for Micro Gas Turbines (MGT) based Energy Applications. *Energy and AI*, **2025**, 20, 100483. https://doi.org/10.1016/j.egyai.2025.100483
48. Bai, M., Yang, X., Liu, J., Liu, J., & Yu, D. Convolutional neural network-based deep transfer learning for fault detection of gas turbine combustion chambers. *Applied Energy*, 2021, 302, 117509. https://doi.org/10.1016/j.apenergy.2021.117509

49. Raissi, M.; Perdikaris, P.; Karniadakis, G. E. Physics-informed neural networks: A deep-learning framework for solving forward and inverse problems involving nonlinear partial-differential equations. *J. Comput. Phys.* **2019**, 378, 686–707. https://doi.org/10.1016/j.jcp.2018.10.045
50. Wu, Y., Sicard, B., & Gadsden, S. A. Physics-informed machine learning: A comprehensive review on applications in anomaly detection and condition monitoring. *Expert Systems With Applications*, **2024**, 255, 124678. https://doi.org/10.1016/j.eswa.2024.124678